Reactive Modified Epoxy Resin and Its Miscible Blends Based on Recycled Oligomers from Solvolysis

Samy Madbouly,* Jose L. Ramos, Wenbin Kuang, Yongsoon Shin, and Kevin L. Simmons*

ABSTRACT: Chemical depolymerization of fully cured epoxy resin with 20% reactive modifier was successfully performed via a solvent-assisted solvolysis process into low molecular weight recyclable oligomers (RO) at 240 °C in a pressure vessel at 650 psi for 4 h. The thermoset epoxy resin was depolymerized into transparent brown viscous fluid with a higher viscosity than the uncured epoxy resin with approximately 93% yield. Different concentrations of the RO were homogeneously mixed with the pure epoxy resin, and their curing kinetics, viscosity, FTIR, mechanical properties, DMA, and cross-link density were investigated. The curing kinetics of the pure reactive modified epoxy resin (baseline) and its mixtures with RO of different concentrations were investigated under both isothermal and nonisothermal conditions using small amplitude oscillatory shear flow. The elastic and viscous moduli (G' and G''), complex viscosity (η^*), and tan δ values were evaluated at different curing times and temperatures. The G', G'', and η^* increased dramatically, while tan δ decreased strongly by several orders of magnitude at the gel point. The zero-shear viscosity (η_0) was determined from the angular frequency dependent on η^* based on the Cross model for different blend compositions in the liquid state before curing. The composition dependence of η_0 showed a positive deviation from the linear mixing rule and was well described by the Lecyar model. The apparent activation energy of curing (E_a) was also evaluated according to the Arrhenius equation and was found to be 46 ± 2 kJ/mol regardless of the different contents of RO. For all blends up to 40 wt % RO, only one tan δ peak systematically shifting to lower temperatures with increasing content of RO was observed in the DMA measurements, indicating that the epoxy resin and the RO are miscible with up to 40 wt % RO.

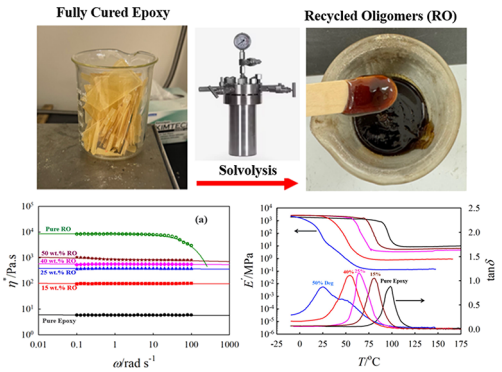

KEYWORDS: *rheokinetics, recycled oligomers, solvolysis, activation energy, mechanical properties, gel time*

INTRODUCTION

High-performance epoxy resin thermosets are extensively used in wide industrial applications due to their excellent chemical and thermal stability, low coefficient of thermal expansion, high glass transition temperature (T_g), high modulus, and high stress at break as well as low viscosity and easy processability into complex shapes.[1−3] A huge volume of epoxy resin thermosets is used annually in the construction and manufacturing of electrical, automotive, and aerospace components, as well as power cables, coatings, adhesives, pressure vessels, encapsulants, and varnishes for magnet wires in electric motors and electric submersible pumps.[4−6] The global thermoset market was valued at $2.5 Bn in 2019 and is expected to reach $5.86 Bn by 2027.[7] Many thermosets can be used continuously at high temperatures and pressures in aggressive environments, as in downhole applications and hydrogen storage (gas and liquid) infrastructure (20 K and 90 MPa). Regardless of the excellent properties and wide applications of commercially available thermosets, they are relatively expensive compared to most thermoplastic polymers, not recyclable, and not biodegradable.

With the huge production and wide industrial applications of thermosetting materials, particularly, the high-temperature glassy epoxy resins, the waste of these nonrecyclable materials is a mounting problem.[8−11] The very stable mechanical, thermal, and chemical properties of the three-dimensional covalent network structure of the thermosets eliminate the possibility of remelting or reprocessing the recyclable resins into products. Developing biodegradable thermosetting materials with similar or better performance than that of petroleum-based thermosets without their drawbacks (nondegradable) is one of the reliable approaches to address this problem.[12−15] According to this recycling approach, the biodegradable thermoset materials can be degraded into CO_2 and water in the soil under landscape

conditions.[16−20] Recently, this approach received great attention and has two main advantages. The first one is to replace petroleum-based thermosetting resins with sustainable biodegradable cost-effective ones. The second advantage is that biobased epoxy resins will significantly reduce the waste of nondegradable epoxy resins and reduce CO_2 emission. However, most of the biobased materials including thermosets have a considerably higher water affinity and lower mechanical properties and are still relatively more expensive than their petroleum-based counterparts.

One different alternative approach for recycling thermoset epoxy resins can be achieved via a mechanical method based on collecting and grinding the recycled materials into fine particles/powders and using them as reinforcement fillers to enhance the mechanical properties and toughness of the pure resin.[11,21] Mixing up to 5 wt % ground recyclable thermoset with pure thermoplastic produced a considerable improvement in the mechanical properties of the resultant composite.[11] Adding a higher content of the recycled thermoset powder to the thermoplastic could negatively impact the mechanical properties due to the aggregation of the recycled powder and the creation of poor interfacial adhesion with the pure polymer matrix.[11] Chemical recycling based on converting the three-dimensional network of the fully cured epoxy resins into their oligomeric structure via the addition of a specific catalyst is the most common recycling process of epoxy resins.[22−25] Therefore, developing new alternative approaches for recycling epoxy waste into high-value products is crucial and will have great significance for the thermoset industry and sustainability.

Covalent adaptable networks (CANs) or malleable thermosets (vitrimers) is also a well-established recycling approach recently used for thermoset polymers via the incorporation of dynamic covalent bonds in the chemical structure of the thermosets.[26−30] According to the relatively new CANs approach, the recycled polymer networks can be reconfigured, remelted, and reshaped into products through a network rearrangement reaction induced by heat, light, or pH. Dissociative and associative mechanisms are commonly involved in the network exchange reaction or CANs. The CANs with dissociative chemical reactions involve a destruction of the network such as a typical reversible Diels−Alder reaction.[31−33] The polymer networks will lose dimension stability and solvent resistance. On the other hand, the polymer network integrity, solvent resistance, and dimensional stability will be maintained with the CANs reactions or vitrimers. Malleability, self-healing, and shape-memory effects are some of the many advantages of CANs. Furthermore, conventional processing techniques, such as compression and injection moldings as well as extrusion, can be used to reprocess vitrimers.

The reactive solvent method is a type of chemical recycling process widely used to break down the covalent bonds in fully cured epoxy resins via a solvolysis process. The solvolysis process is a chemical recycling process of epoxy resins based on a solvent-assisted process that allows depolymerization of the fully cured resins into their monomers or oligomers. The solvolysis process strongly depends on the nature of the solvent, catalyst, temperature, pressure, and processing time.[34−38] A typical solvolysis process can be achieved with supercritical/near-supercritical fluids or with specific catalysts under mild conditions (e.g., low temperature and pressure). Water and low molecular weight ketones and alcohols (e.g., acetone and methanol) are common solvents used for the cost-effective solvolysis process of epoxy resins under supercritical conditions and very high pressure.[39,40] The solvolysis process can be carried out at atmospheric pressure and low temperatures, lower than 200 °C with a considerable increase in the rate of the solvolysis process by adding specific catalysis. This mild temperature and atmospheric pressure condition required a large amount of expensive and flammable solvents and specific catalysis. In addition to the above-mentioned parameters, the success of the solvolysis process greatly depends on the chemical structure of the resin, the nature of hardeners, coupling agents, and chemical modifiers. Fully cured epoxy with amine hardeners was depolymerized into monomers or oligomers via a catalyzed solvolysis process at a temperature <200 °C in a pressure vessel.[41] Transesterification between hydroxyl groups of the solvolysis solvent and ester groups in the epoxy resin leads to depolymerization of the anhydride-cured epoxies.[42−44] Depolymerization of epoxy resins into monomers or oligomers particularly with catalysis under mild temperature and pressure via the solvolysis process has a significant importance in the recycling process of carbon fiber (CF) epoxy resins.[45] The solvolysis process provides a unique practical approach to depolymerize the epoxy resin matrix into low molecular weight monomers or oligomers that can be reused or mixed with pure epoxy resin to fabricate thermosetting products. Another more important advantage of the solvolysis process is the recycling of the high-performance CF with no significant damage in the CF diameter, length, and surface roughness.[37,40,46−49] The recycled CF from the solvolysis process of CF-reinforced epoxy resin can be used for many other applications, which can significantly reduce the excessive energy commonly used to fabricate CF and reduce the CO_2 emission associated with the synthesis of the CF. Therefore, developing the solvolysis process and creating catalysts to improve the performance under mild conditions (low temperature and pressure) could be very crucial with practical, industrial, and environmental importance that will have a significant positive impact on the future of the CF and epoxy resin recycling industries.

A fundamental understanding of the curing kinetics of thermosetting materials is very crucial to control the mechanism of macroscopic gelation (structure and formation of three-dimensional networks) and the mechanical properties (tensile strength, toughness, elongation at break, etc.) of the final thermosetting products. It also provides critical information for optimizing the processing conditions as well as the performance of the final products. The curing kinetics of thermosetting materials have been investigated in the last decades, although there are still controversial topics due to the complexity of the curing reactions and the insolubility of the products at different degrees of conversion.[50,51] Many different experimental techniques were previously employed for investigating the curing kinetics of thermosets including DSC (differential scanning calorimetry),[52] FTIR (Fourier transform infrared spectroscopy),[53] ^{13}C NMR (nuclear magnetic resonance),[54] mechanical characterizations,[55] dynamic rheology, and others.[56] Swelling ratio experiments do not provide any useful data related to the curing kinetics and therefore are not suitable for evaluating the optimal cross-linking reaction and controlling the desired properties.[57] Also, curing the sample isothermally at different time intervals followed by measuring the T_g or mechanical properties has the drawback of being not able to investigate the curing kinetics and determine the gel time.[58] Dynamic rheology is one of the few techniques capable of evaluating the gel time and accurately studying the curing kinetics of thermosets at different curing times, angular

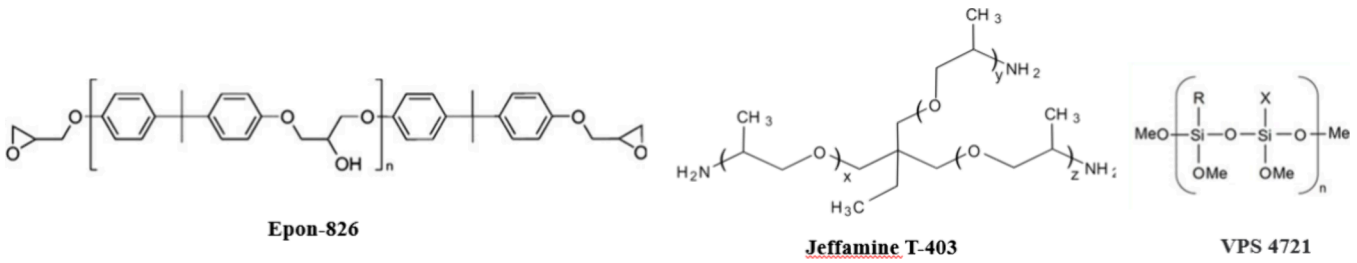

Figure 1. Chemical structures of the epoxy resin (Epon 826), hardener (Jeffamine), and silane coupling agent (VPS) used in this work. The NANOPOX F 400 reactive modifier is an epoxy resin with silica nanoparticles.

frequencies, and strain rates. It is widely used to evaluate the curing kinetics of physical and chemical cross-link reactions by monitoring the changes in the material microstructure and viscoelastic materials functions (G', G'', η^*, and tan δ) during the gelation process. Dynamic rheology commonly evaluates the curing kinetics of cross-link reactions using small-amplitude oscillatory shear flow in the linear viscoelastic regime with no disruption of the microstructure of the networks. The viscoelastic properties of the cross-link polymers in the vicinity of the sol−gel transition have been studied experimentally and theoretically to understand the relationship between the gel structure and linear viscoelastic behavior.[59,60]

In this manuscript, the solvolysis process of epoxy resin with 20% reactive modifier and 1% coupling agent was investigated at 240 °C in a pressure vessel at 650 psi for 4 h as a potential chemical recycling process. The obtained RO was mixed without any chemical modification with pure epoxy resin with different concentrations to utilize its application in creating thermoset materials. The effect of the RO on the viscosity, curing kinetics, and mechanical and thermomechanical properties were thoroughly investigated. The rheological parameters G', G'', η^*, and tan δ were evaluated as a function of curing time, temperature, and angular frequency. The real-time measurements of the viscoelastic properties during the curing process at a constant temperature and angular frequency near the gel temperature (T_{gel}) were also studied. The FTIR of the RO and their blends with the pure resins were studied. The mechanical and thermomechanical properties of the fully cured mixture of epoxy resins and recycled oligomers were investigated using an Instron machine and DMA, respectively. The apparent activation energy of curing was also evaluated from the temperature dependence of gel time (t_{gel}) according to the Arrhenius Equation.

EXPERIMENTAL SECTION

Materials. EPON Resin 826 is a bisphenol A based epoxy resin obtained from Westlake Corporation. The EPON Resin 826 is a low-viscosity light-colored liquid that can be fully cured with a wide range of hardeners to produce a high-strength thermoset with excellent chemical resistance. NANOPOX F 400 (Evonik Industries AG) is a high-performance, silica-reinforced epoxy resin commonly used as a reactive modifier with 40 wt % SiO_2 content. Despite the high SiO_2 content, NANOPOX F 400 has a comparatively low viscosity due to the agglomerate-free colloidal dispersion of the nanoparticles (20 nm) in the resin. JEFFAMINE T-403 polyether amine is a highly reactive trifunctional primary amine curing agent obtained from Huntsman Corporation. Organofunctional silane additive (VPS 4721) has an epoxy-functional silane oligomer obtained from Evonik Industries AG and is used with 1.0 wt % to improve the compatibility between EPON Resin 826, NANOPOX F 400, and JEFFAMINE T-403. The chemical structures of the three materials used in the formulation of the control-based epoxy resin can be found in Figure 1.

Sample Preparation. The control-based epoxy resin formulation was prepared by mixing EPON Resin 826 with 20 wt % reactive modifier (F-400), 1.0 wt % silane additive (VPS 4721), and 46 phr JEFFAMINE T-403 polyether amine hardener. Because the RO does not have any reactive epoxy groups, the composition of the hardener was kept constant at 46 phr regardless of the content of RO. The obtained blend was homogeneously mixed using a Mazerustar planetary mixer at room temperature and 1000 rpm for 3 min. The mixture was then degassed under a vacuum for another 15 min to obtain a clear mixture with free air bubbles. The mixture was then cast into a metal mold and cured at 100 °C for 3 h followed by 2 h at 150 °C. Both DSC and DMA were run after the just mentioned curing process. No exothermic peak was observed in the DSC thermogram. In addition, the storage modulus and T_g from the temperature at the peak maximum of tan d of the DMA data did not change after the second run of the test at −20 to 200 °C. The fully cured sample was then machined into dog bone specimens for mechanical measurements and rectangular shape specimens for DMA (3 mm thick, 12 mm width, and 30 mm length) measurements using a Wazer Waterjet. Clear-cut with no microcracks was obtained for both mechanical and DMA specimens using the Wazer Waterjet machine.

Solvolysis Process. The solvolysis process was carried out for a fully cured epoxy resin under the above curing conditions. The fully cured sample was cut into small pieces and heated in a pressure vessel at 240 °C for 4 h in a solution consisting of 70% water, 20% zinc acetate, and 10% acetic acid.[61,62] The zinc acetate is acting as a catalyst for the solvolysis process. The acetic acid was found to be suitable for the depolymerization of epoxy resins with amine hardeners via the breaking of carbon−nitrogen bonds. It also has a Hansen solubility parameter close to that of amine-cured epoxy resin and thereby can swell the CFRP to facilitate the decomposition of the matrix polymer.[49] The pressure built up during this solvolysis process was measured as 650 psi. The recycled oligomers obtained from the solvolysis process were washed with DI water several times and dried in a vacuum oven at 60 °C for 24 h. The obtained recycled oligomers (RO) are transparent brown, viscous liquids. The solvolysis process used in this study was very efficient in depolymerizing a high-cross-link epoxy resin into oligomers with approximately 94% yield.

Rheological Measurements. The curing kinetics were investigated for the pure epoxy resin and epoxy/RO blends of different RO contents (15, 25, 40, and 50 wt %) obtained from the solvolysis process as described above. The rheological curing kinetics were investigated using a TA Instruments (AR2000EX) instrument with 25 mm diameter parallel plates. All isothermal and nonisothermal rheological curing kinetics measurements were investigated under thermal conditions of ±0.1 K. The following experiments were performed:

1. Strain sweep at a constant angular frequency to obtain the linear viscoelastic regime at a constant temperature for each mixture.
2. A temperature sweep from 20 to 170 °C at 2 °C/min under a constant angular frequency and 1% strain rate in the linear viscoelastic regime to evaluate the temperature of gelation.
3. Real-time sweep measurements at different constant gelation temperatures in the linear viscoelastic regime to investigate the effect of the curing process on the different viscoelastic characteristic functions including storage moduli (G' and G'') as well as η^* and tan δ.

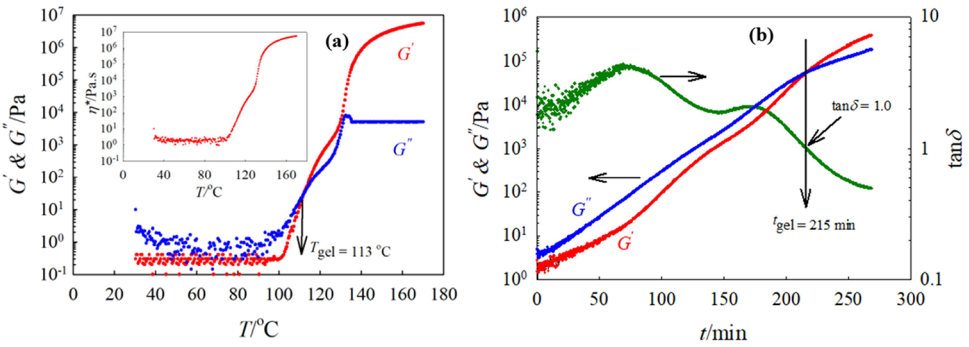

Figure 2. (a) Temperature dependence of G' and G'' at 1 rad/s and 1% strain rate in the linear viscoelastic regime. The inset plot illustrates η^* at different temperatures. The measurements were carried out at a 2 °C/min heating rate. (b) Curing time dependence of G', G'', and tan δ at 1 rad/s and 1% strain rate in the linear viscoelastic regime. The arrows show the t_{gel} = 215 min and tan δ = 1.0 at the t_{gel}.

4. The activation energy of curing was evaluated from the temperature dependence of gel time according to the Arrhenius equation.
5. The composition dependence of RO on the η^* was theoretically described based on the Lecyar model.

FTIR, Mechanical, and DMA Measurements. Fourier transform infrared spectroscopy (FTIR) was studied for pure RO viscous material and fully cured blends with epoxy resins of different concentrations. The measurements were carried out using a Thermo Scientific Nicolet iSTM 10 FTIR spectrometer based on attenuated total reflectance (ATR) absorbance mode using a Harrick diamax with a diamond ATR crystal. A total of 128 scans were collected and the resolution was 0.482 cm^{-1}.

The dynamic mechanical analysis (DMA) measurements of different fully cured epoxy/RO blends were carried out using a Q800 dynamic mechanical analyzer. Three-point bending tests for rectangular-shaped samples of approximately 3.0 mm thickness, 30 mm length, and 12 mm width were investigated from −20 to 200 °C at a 3 °C/min heating rate and 1 Hz frequency under a nitrogen atmosphere. The DMA measurements were employed to evaluate the glass transition temperature (T_g) from the temperature at the peak maximum of tan δ. The storage modulus at low temperatures, lower than the T_g, and the cross-link density of the different epoxy/RO blends were also evaluated.

The tensile properties were carried out using an Instron machine 5582 according to the ASTM D638 method at a 5 mm/min strain rate. Five samples were measured for each blend composition. A high-resolution noncontact laser extensometer was used for accurately evaluating the elongation at break for marked dog bone specimens.

RESULTS AND DISCUSSION

Curing Kinetics of Baseline. The viscoelastic properties at the gel point have universal fundamental behavior due to the change in molecular weight, chain length, molecular dynamics, mechanical properties, etc. Real-time investigation of G', G'', η^*, and tan δ at a temperature range in the vicinity of the gel point is one of the most accurate methods commonly used to evaluate the gel point and monitor the progress of the gelation process from the sudden increase in the viscoelastic parameters at the onset of the gelation process. The molecular weight increases dramatically at the gel point, and the material loses its flow even at high temperatures. At the gel point, a huge increase in the molecular weight of the material is normally expected, where the existence of one long chain running through the whole system with a sudden loss of flow is the most common criterion of gel formation.

Figure 2a shows the temperature dependence of G' and G'' for the control sample at 1 rad/s angular frequency in the linear viscoelastic regime (1% strain) at a 2 °C/min heating rate. At a low-temperature range lower than the gel temperature (T_{gel}), the G'' is higher than the G', indicating that the sample has a liquid-like behavior. The G' and G'' curves cross over at T_{gel} = 113 °C. After that, both G' and G'' increased dramatically with increasing temperature but G' increased greatly and became significantly higher than G''. At very high temperatures in the late stage of the curing process, the elevation of both G' and G'' was less temperature dependent due to the formation of an equilibrium storage modulus (G_{eq}), a typical criterion for a cross-linked structure. The inset plot of Figure 2a demonstrates the η^* as a function of temperature at 1 rad/s angular frequency and 1% strain. The η^* behaved with temperature very similar to the temperature dependence of G' and G'' (i.e., the η^* was not significantly changed at a temperature range lower than T_{gel} and dramatically increased above T_{gel}).

Accurately evaluating the value of T_{gel} from Figure 2a enables us to investigate the curing kinetics from real-time measurements of the viscoelastic material functions at different curing temperatures in the vicinity of the T_{gel}. The lower the curing temperature, the longer the curing time and the higher the gel time (t_{gel}). The t_{gel} can be evaluated from the crossover time of G' and G'' at a constant temperature and an angular frequency in the linear viscoelastic regime. Figure 2b shows the curing time dependence of G', G'', and tan δ at 55 °C. Clearly, G'' is higher than G' at the time range lower than the t_{gel} and both of them increased significantly with increasing the curing time at 55 °C. At t_{gel} = 215 min, the G' and G'' crossover, and G' increased more rapidly and became significantly higher than G''. It is also clear from Figure 2b that there are two curing processes involved in the cross-link reaction of this system. The first curing reaction was started early at the beginning of the process up to 170 min at 55 °C. In this curing stage, both G' and G'' increase dramatically (approximately 4 orders of magnitude), but still G'' is higher than G' (liquid-like behavior). The second curing process starts at a longer time, where G' and G'' still increase with curing time and coincide at t_{gel} = 215 min, and G' increases more rapidly than G'' due to the formation of three-dimensional networks. The two curing processes can be observed in the time dependence of the tan δ value of Figure 2b. The two processes were observed as two peaks in the tan δ curve at 75 and 175 min, respectively. The two processes are involved in the progress of the cross-link reaction, but the time to complete the first process is not enough to generate a gel structure and it only covers the initial stage of the curing process. During the first process, a considerable increase in viscosity, G', and G'' was observed without the formation of a network structure or before reaching the gel point. The second process is a continuation of the first cross-link reaction, and the gel point was observed from the

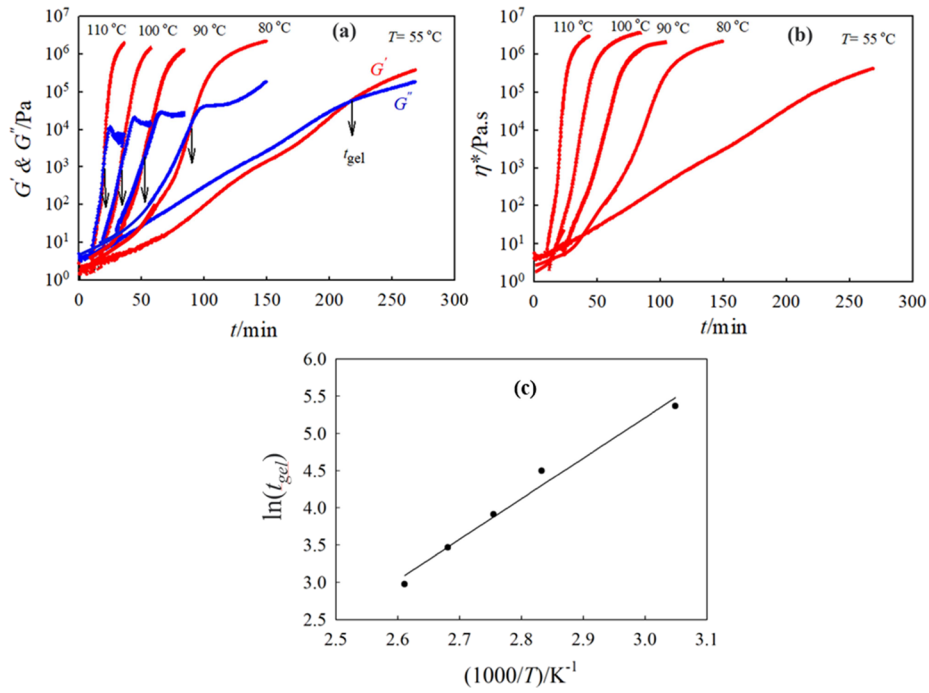

Figure 3. (a) Curing time dependence of G' and G'' at different constant curing temperatures (the t_{gel} = 215 min obtained from the crossover points of G' and G'' as shown by the arrow). (b) Curing time dependence of η^*h^* at different constant curing temperatures. (c) Absolute inverse temperature $(1/T)$ dependence of t_{gel} for the isothermal gelation process of the control epoxy system. This figure is for the control sample.

crossover point of G' and G'' at 215 min as mentioned above. At the t_{gel}, tan δ = 1.0, as shown by the arrow in Figure 2b. At curing times longer than the t_{gel}, the curing reaction proceeds, and the formation of three-dimensional polymer networks is characterized by $G' > G''$. Furthermore, the values of G' and G'' reach near-equilibrium or become less curing time dependent.

The curing kinetics and activation energy of the curing process can be studied from the values of t_{gel} at different constant temperatures. Figure 3a shows the curing time dependences of G' and G'' at different curing temperatures. Obviously the higher the curing temperature, the shorter the t_{gel}, where the curing reaction accelerated greatly by increasing the curing temperature. For example, the t_{gel} at 55 °C is 215 min, while the value of the t_{gel} at 110 °C is about 19 min, as clearly shown by the arrows in Figure 3a. The crossover point between elastic and viscous moduli at a constant angular frequency is identical to the point obtained from the multifrequency mode according to the Chambon and Winter method. The obtained data are in good agreement with t_{gel}, previously determined from the point of intersection in tan δ vs gelation time over a wide range of angular frequency, where tan δ was found to be independent of angular frequency and all curves cross over, according to the Winter–Chambon criterion. The value of t_{gel} obtained from the coincidence of G' and G'' was in excellent agreement with that obtained from the Winter–Chambon method for thermal-induced gelation of water-based polyurethane dispersion.[51]

The η^* at different isothermal curing temperatures showed behavior similar to that of G' and G'' in Figure 3b. The η^* increased dramatically with increasing curing time and reached a near equilibrium stage, at which the viscosity increased by about 6 orders of magnitude and became less curing time dependent. The near-equilibrium value of η^* is strongly dependent on curing temperature and curing time. The higher the curing temperature, the shorter the time required for the viscosity to reach the near-equilibrium value (approximately 5×10^6 Pa·s).

Based on the preceding discussion, it appears that the rheological parameters including G', G'', η^*, and tan δ of the current system are very sensitive to the formation of chemically cross-linked structures and the curing kinetics can be evaluated rheologically. The curing kinetics of the thermal-induced cross-link reaction can be investigated by determining the apparent activation energy (E_a).[65] This method is based on determining a single value of activation energy for an overall process and neglecting the effect of changes in the reaction mechanism and degree of conversion at different temperatures. This approach is widely used in literature, and the value of E_a can be determined according to Arrhenius equation:[65]

$$\ln(t_{gel}) = \text{constant} + \frac{E_a}{RT} \quad (1)$$

where R is the universal gas constant and T is the absolute curing temperature. The value of E_a can be simply calculated from the slope of the linear relationship between $\ln(t_{gel})$ and the inverse of the absolute temperature $(1/T)$, as seen in Figure 3c. The obtained E_a for this system was 44.7 kJ/mol, very close to the activation energy of many other thermosetting systems reported in the literature and calculated according to the Malkin and Kulichikhin model, isoconversional method, and model-free kinetics.[66,67]

Recycling Process of Epoxy Resin. The successful recycling process of epoxy resins used in the winding process of CF is a very crucial and required step for recycling the expensive and energy-intensive CF. The fully cured aliphatic amine-based (Epon826–20%F400–1% VPS–T403) formulation was cut into small pieces and then depolymerized via solvolysis in a solution of water, zinc chloride, and acetic acid at 240 °C in a pressure vessel, as mentioned in the Experimental section. We successfully depolymerized the fully cured epoxy resin into a RO viscous liquid as shown in Figure 4.

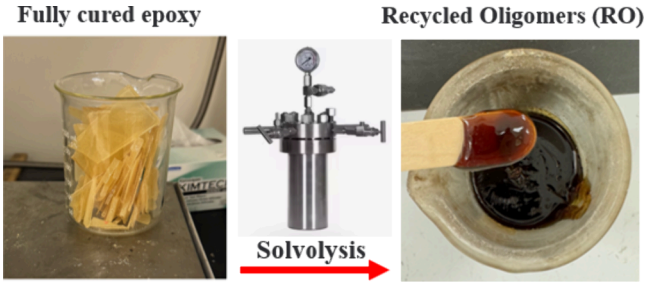

Cured epoxy/g	RO/g	Yield%
56.95	54.33	95.4
24.62	48.98	89.7
111.73	104.36	93.4
108.55	102.97	94.8
Average		93.3

Figure 4. Pictures of the fully cured epoxy and its recycled oligomers (RO) from the solvolysis process. The table summarizes the number of samples of the crushed epoxy, their weight in comparison with the amounts of RO of each sample, and their yield %.

The RO was washed with DI water and dried at 60 °C for 15 h in a vacuum oven. The yield of RO reached an average of 93.3% (see the table in Figure 4). The FTIR result for RO exhibited strong fully cured epoxy peaks and high oxidation peaks. To evaluate the utilization of the RO in the manufacturing of thermosetting materials, the RO was mixed with pure epoxy resin with different concentrations, namely 15, 25, 40, and 50 wt % RO. The obtained blends were homogeneously mixed with the hardener at room temperature using a Mazerustar planetary mixer and fully cured according to the curing schedule described in the Experimental section.

The FTIR was performed for the blends of epoxy/RO of different concentrations. According to the FTIR data shown in Figure 5, the pure RO (viscous liquid) showed the highest intensity for the FTIR oxidation peak obtained from the carbonyl index. The blends of the RO with the pure epoxy showed a lower intensity of the oxidation peak based on the different contents of the RO; the higher the content of RO the higher the intensity of the oxidation peak. The pure epoxy without any RO showed the lowest intensity peak for oxidation. The oxidation occurs during the depolymerization process, and this is why the pure RO has the highest oxidation compared to that of the pure epoxy. The FTIR stretching epoxy peak, ν(C−O), was also evaluated and found to be strongly dependent on the content of the RO. The blends with lower contents of RO have higher epoxy curing contents according to the epoxy peak intensity ratio shown in Figure 5a. The FTIR data are also summarized in Figure 5b, where the carbonyl and epoxy peak intensities were evaluated and demonstrated as a function of blend compositions. The original or pure epoxy resin showed the minimum carbonyl peak intensity. The carbonyl group intensity of the pure RO is the maximum and decreases gradually with decreasing content of RO. In addition, the epoxy curing peak intensity was also the maximum for the RO and decreased dramatically for pure resin and slightly increased with increasing content of RO. No uncured epoxy peaks were detected, and no free amine groups were observed in the FTIR spectrum as shown in Figure 5.

Viscosity of Epoxy/RO Uncured Blends. The effect of RO on the flow behavior and viscosity of uncured epoxy resin must be investigated to understand the processing behavior and applications of recycled/epoxy blends. The η^* of the uncured epoxy/RO blends (no hardener) as a function of angular frequency for different RO contents at 20 °C are depicted in Figure 6a. The η^* of the pure epoxy resin increased significantly with increasing content of RO. It is also obvious that the η^* of the RO is about 3 orders of magnitude higher than that of the pure epoxy at the same temperature and angular frequency. All of the blends of different RO concentrations showed Newtonian behavior over the entire range of angular frequency (i.e., η^* is constant regardless of the different values of the angular frequency). For pure RO, the complex viscosity showed Newtonian behavior at low angular frequencies ranging up to 25 rad/s and then decreased considerably at high values of angular frequency (non-Newtonian behavior). The angular frequency dependence of η^* for epoxy/RO blends of different contents at 20 °C can be described by the Cross model:[68]

$$\eta^* = \frac{\eta_0}{1 + \left(\frac{\omega}{\omega_c}\right)^{\beta}} \tag{2}$$

where η_0 is the zero-shear viscosity, β is a material constant depending on the nature of the blend composition, and ω_c is the critical angular frequency, which can be evaluated from the point at which the η^* decreases to its half initial value. The Cross model (eq 2) was employed to evaluate η_0 as a fitting parameter to the experimental data of Figure 5a. The solid lines in Figure 6a were computed from the Cross model using η_0, β, and ω_c as fitting parameters. The experimental data were found to fit well with the Cross model.

The epoxy/RO blends with different compositions showed homogeneous mixtures with no phase separation (i.e., visually clear, and no morphology was observed under an optical microscope). Based on the FTIR data in Figure 5, the RO has no unreacted epoxy groups; therefore, the epoxy/RO blends will not copolymerize but will form semi-interpenetrating networks as one blend component (epoxy resin) and will thermally cure at high temperature by adding a hardener. The other component (RO) will act as plasticizer with no contribution in the curing reaction, which might decrease the cross-link density and T_g of the fully cured epoxy resin. The effect of RO on the mechanical and thermomechanical (DMA) properties, as well as the cross-link density, will be studied in the next section.

The composition dependence of η_0 obtained from fitting the experimental data of Figure 6a to the Cross model is shown in Figure 6b. As just mentioned, the epoxy resin/RO can be described using a miscible polymer mixtures equation, such as the Lecyar model:[69]

$$\ln \eta_b = A w_1^3 + B w_2^3 + C w_1^2 w_2 + D w_1 w_2^2 \tag{3}$$

where η_b is the η_0 of the blend and w_1 and w_2 are the weight fractions of epoxy resin and RO, respectively. The constants A−D are material parameters that depend on temperature and angular frequency. The composition dependence of η_0 obtained from fitting the experimental data in Figure 6a to the Cross model is shown in Figure 6b. The symbols are the experimental data, and the solid line was calculated from the Lecyar model. An excellent description of the data was obtained by the Lecyar mode. The dashed line demonstrates the linear rule obtained from eq 4:

$$\ln \eta_b = w_1 \ln \eta_1 + w_2 \ln \eta_2 \tag{4}$$

where η_1 and η_2 are the zero-shear viscosity of epoxy and RO, respectively. The linear relation described by the dashed line

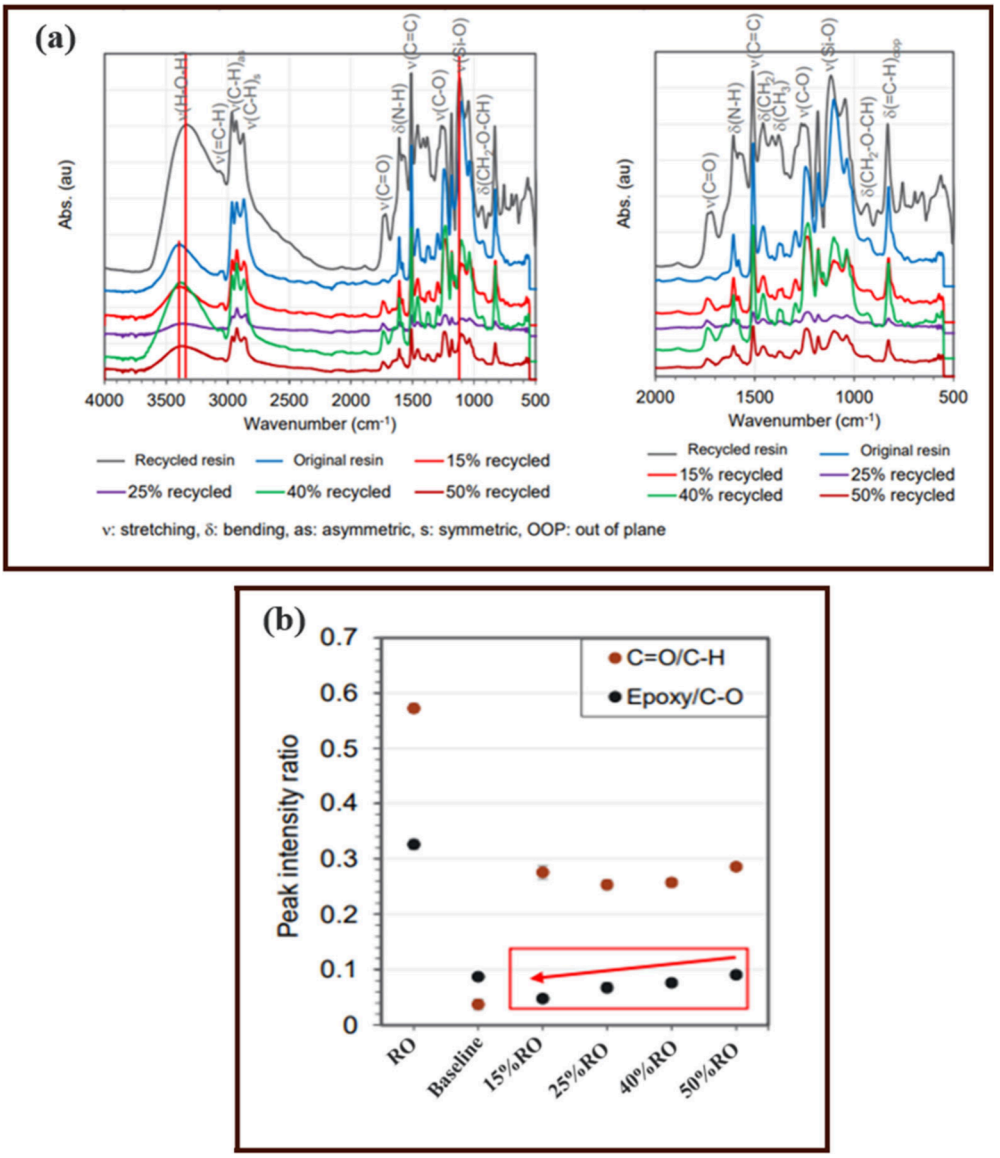

Figure 5. (a) FTIR spectrum of recycled oligomers/epoxy resin blends and their stretching epoxy and carbonyl peak intensities as a function of blend composition. (b) FTIR peak intensities for C=O/C−H and cured epoxy/C−O of different compositions.

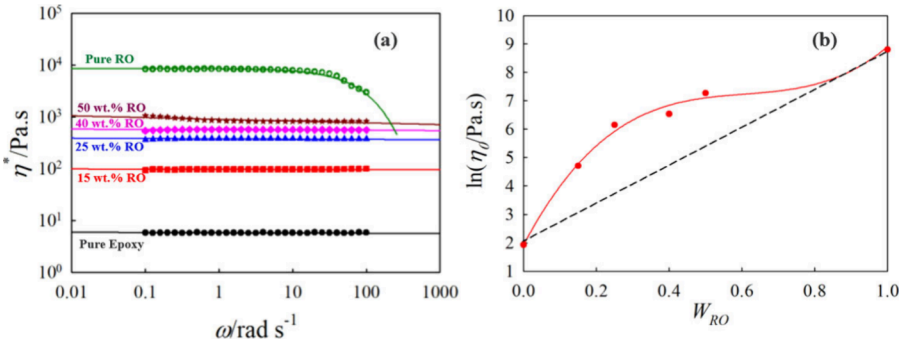

Figure 6. (a) Angular frequency dependence of η^* for epoxy/RO blends at 20 °C (uncured blends). The lines are computed from the cross model. (b) η^* as a function of the weight fraction of RO at 20 °C. The line is computed from the Lecyar model (eq 3). The dashed line shows the linear behavior (eq 4).

shows how the experimental data greatly deviated from the linearity in a semilogarithmic scale. The positive deviation from the linear mixing rule might suggest that the mixtures of the uncured epoxy with RO have a strong physical interaction compared to the common miscible thermoplastic polymer blends in the melt state. The effect of RO on the curing kinetics and mechanical and dynamic mechanical thermal analysis (DMA) will be investigated in the next section.

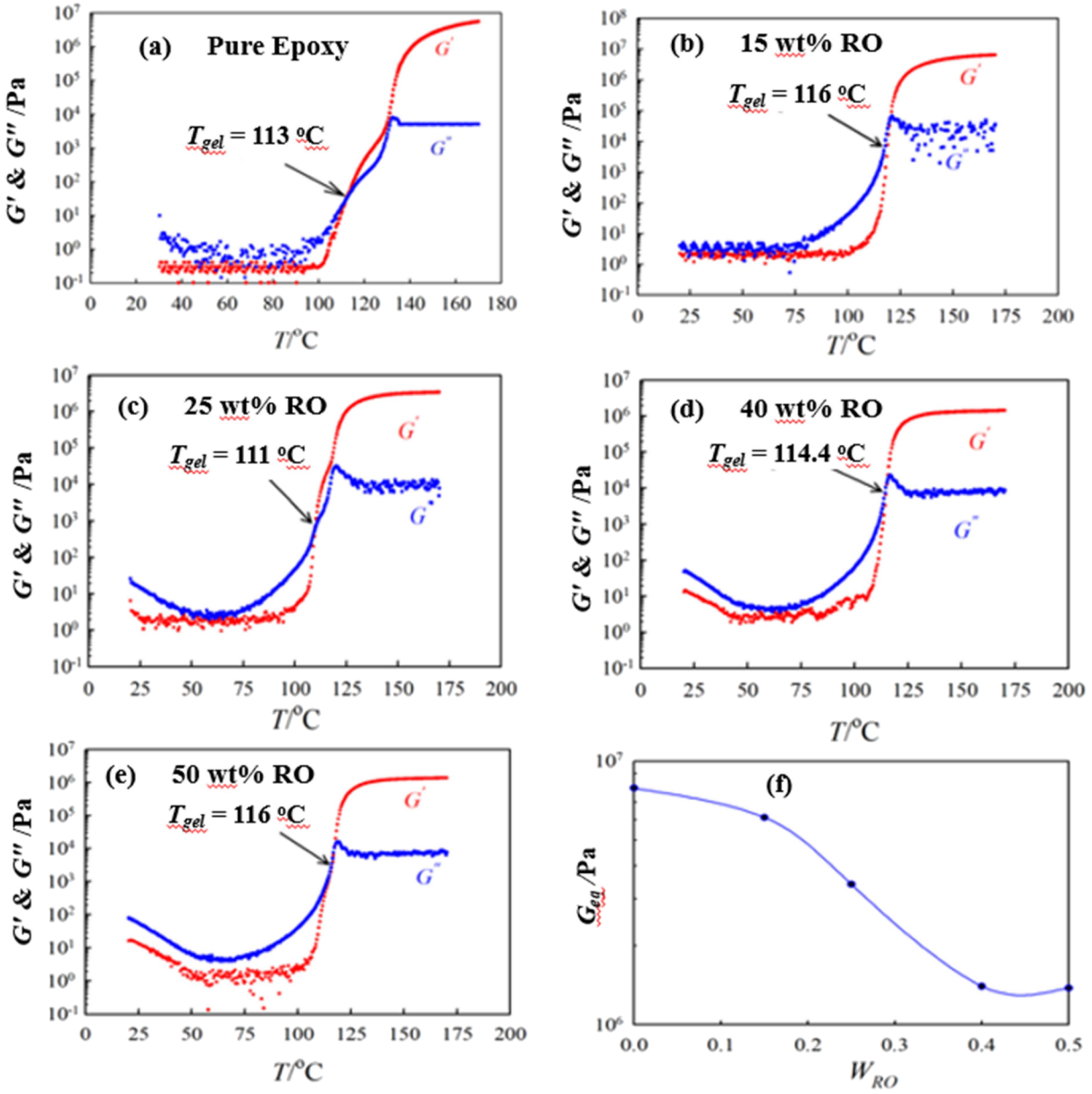

Figure 7. Temperature dependence of G' and G'' for epoxy/RO blends with different contents: (a) pure epoxy, (b) blend with 15 wt % RO, (c) blend with 25 wt % RO, (d) blend with 40 wt % RO, and (e) blend with 50 wt % RO. The arrows show the value of T_{gel} for each blend composition. (f) Composition dependence of G_{eq}.

Effect of RO on the Curing Kinetics and Mechanical and Thermomechanical Properties. To study the effect of RO on the curing kinetics of epoxy resin, the RO with different contents mixed with pure resin and hardener; after that, the nonisothermal curing kinetics were investigated rheologically by measuring the dynamic G' and G'' at 1 rad/s angular frequency and 1.0% strain at 2 °C/min heating rate. The T_{gel} values obtained from the crossover point of G' and G'' for the blends of different concentrations were in the range of 111−116 °C. This change in the value of T_{gel} with different concentrations of RO is mainly because the T_{gel} is not a single value from the crossover point of G' and G'', but the overlap between G' and G'' occurred over a temperature range at which G' and G'' coincided, as clearly seen in Figure 7. For example, the overlap between G' and G'' was observed at a temperature range of 110 to 114 °C for pure epoxy resin. Therefore, we can conclude that the impact of RO on the T_{gel} and curing kinetics is not significant. The equilibrium elastic modulus, G_{eq} obtained from the plateau of the G' at high temperature (e.g., 170 °C) was evaluated from Figure 7. The G_{eq} decreased with increasing the content of RO. It is also clear that the G_{eq} decreased slightly at low and high concentrations of RO (15 and 50 wt %), while it decreased dramatically in the 25 and 40 wt % concentration range, as seen in Figure 7f. This considerable decrease in the G_{eq} with increasing the concentration of RO in the blend also indicated that the RO has no reactive epoxy groups and can act as a plasticizer to decrease the cross-link density and not copolymerize with the pure epoxy resin. The isothermal curing kinetics at different constant curing temperatures for the epoxy resin/RO blends was investigated, and the E_a was evaluated. The $E_a = 46 \pm 2$ kJ/mol regardless of the contents of RO. This data is in good agreement with the nonisothermal curing kinetics just mentioned above and described in Figure 7. Based on this find, it appears that both isothermal and nonisothermal curing kinetics

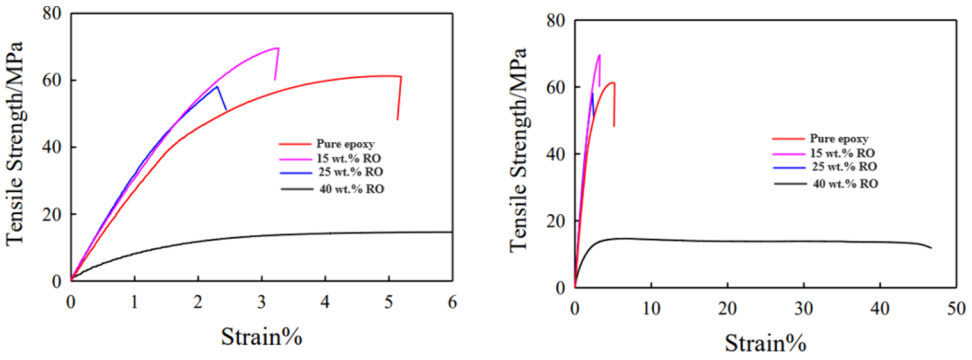

Figure 8. Stress−strain curves for fully cured epoxy resin/RO blends with different contents of RO.

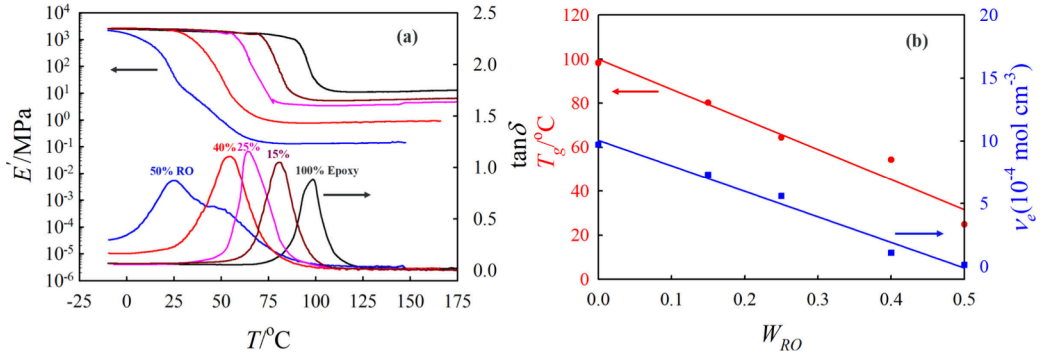

Figure 9. (a) Temperature dependence of E' and tan δ for epoxy resin/RO blends with different contents of RO at 1 Hz with a 2 °C/min heating rate. (b) Dependence of T_g and cross-link density (υ_e) on the content of RO for epoxy resin/RO blends.

have no significant impact by adding different contents of RO to the baseline epoxy resin. The effect of RO on the mechanical properties of the epoxy resin was also investigated. The content of the RO was strongly influenced by the mechanical properties of the pure epoxy resin, as shown in Figure 8. Significant increases in the modulus by 40% and 20% were observed for epoxy resin/RO blends with 15 and 25 wt % RO, respectively. An increase in the tensile strength by 17.5%, a decrease by −5.9%, and a decrease in the elongation by −49% and −61% were also observed for the same blend concentrations (15 and 25 wt % RO, respectively). Based on the above, the blends with 15 and 25 wt % RO have a promising mechanical behavior that can be improved with reactive modifiers or coupling agents to be comparable to or exceed the baseline (pure epoxy). Low contents of RO up to 25% in the epoxy/RO blends showed a higher modulus than the pure epoxy. This is not a common behavior, but it has been reported many times in different systems in the literature. The behavior is related to the strong physical interaction between the components of the polymer blend. This strong physical interaction can also create polymer blends with T_{gs} values higher than those of the pure components. For example, an increase in the modulus by approximately 6% was observed in the PMMA/PLA blends. The tensile strength of the blend (PMMA/PLA) showed an 11% increase compared to the pure blend components.[63] A positive deviation from the linear mixing rule of composition dependence of T_g was also observed for poly(ether imide)/polybenzimidazole and PMMA/cellulose acetate hydrogen phthalate. The behavior was attributed to the strong physical interaction between the polymer components.[64] Therefore, the increase in the modulus and stress at break for epoxy/RO with 15% and 25% RO is not surprising at all. The epoxy resin/RO blend with 50 wt % RO was very soft and sticky, so we could not perform the machinal tests for this blend. The blend with 40% RO was successfully prepared, and we could measure the mechanical properties of this blend. We found that the modulus and tensile strength decreased dramatically from 3000 and 60 MPa for pure epoxy resin (baseline) to 1300 and 14.5 MPa for the blend with 40 wt % RO, respectively. However, on the other hand, the blend with 40 wt % RO showed a dramatic increase in elongation from 6% for pure epoxy resin to about 42% elongation for the blend. The high concentration of the RO leads to a considerable decrease in the T_g and the cross-link density (see next section) and greatly improves the flexibility and decreases the modulus and strength, as mentioned above. These data suggested that the RO does not react chemically or copolymerize with the epoxy baseline, but it acts as a good miscible plasticizer that improves the strain at break and decreases the T_g and tensile strength.

The DMA for fully cured blends of epoxy resin/RO of different contents was also investigated over a wide range of temperatures (−20 to 200 °C) at 1 Hz with a 3 °C/min heating rate. Figure 9a shows the temperature dependence of the storage modulus (E') and tan δ. One can see that, for all blends except the 50 wt % RO, only one tan δ peak systematically shifted to lower temperatures with increasing content of RO. The systematic shifting to lower temperature in the tan δ peak maximum with increasing the content of RO indicates that the epoxy resin and the RO are miscible with up to 40 wt % RO. For the 50 wt % blend, two tan δ peaks were observed, one at about 50 °C and the other one at 25 °C. The observation of two tan δ peaks for the 50% RO blend suggested that there is a phase separation between epoxy resin and RO. The storage modulus of all blends is the same at the low-temperature range, lower than the glass relaxation process, in the glassy state below the T_g. This observation is very useful for the applications of these blends at a low-temperature range, in the glassy state, below the T_g where

Table 1. Mechanical Properties and Other Parameters of Epoxy Resin/RO Blends with Different Concentrations of RO

RO (%)	η_0 (Pa·s)	T_g (°C)	υ_e mol m^{-3}	G' (MPa) (125 °C)	G_{eq} (MPa) (170 °C)	T_{gel} (°C)	E_a (kJ mol^{-1})	mod. (MPa)	TS (MPa)	elong. (%)
0	6.9	98.3	9.7	1.73	7.6×10^6	113	46	2950	60.5	6
15	110	80.2	7.3	1.45	5.5×10^6	116	48	4150	71	2.9
25	469	64.4	5.6	1.61	3.1×10^6	111	44	3600	56	2.2
40	686	54.3	1.1	1.66	1.4×10^6	114	47	1300	13	42
50	1431	24.8	0.15	1.2	1.2×10^6	116	48	-	-	-
100	8673	-	-	-	-	-	-	-	-	-

the RO has no significant impact on the stiffness of the blends in this low-temperature range. The T_g can be obtained from the temperature at the peak maximum of tan δ, which decreases linearly with increasing content of RO, as seen in Figure 9b (presenting only one T_g at 25 °C for the 50 wt % blend).

The plateau storage modulus at high temperatures above the tan δ peak decreased significantly with increasing the content of the RO. The cross-link density can be determined from the plateau modulus of E' at 45 °C above the T_g according to the rubber elasticity theory, as described in the following equation:[70]

$$E' = 3\upsilon_e RT \tag{5}$$

where υ_e is the cross-link density, E' is the storage modulus at 45 °C above the T_g of each blend composition, R is the universal gas constant, and T is the absolute temperature. The cross-link density of the pure epoxy decreases linearly with increasing content of RO. The data of the 15 and 25 wt % blends still showed one phase structure with one T_g and good cross-link density that can be developed to exceed the corresponding values of the baseline by adding a small amount of reactive modifier and/or a coupling agent blend, which will be the topic of our next publication. The mechanical properties (modulus, tensile strength, and elongation at break), T_g, T_{gel}, E_a, υ_e, E' (at 10 °C), and η_0 for epoxy resin/RO blends of different concentrations of RO are summarized in Table 1.

CONCLUSION

A chemical depolymerization of fully cured epoxy resin with a 20% reactive modifier and 1% coupling agent was successfully achieved via a solvent-assisted solvolysis process at 240 °C and 650 psi for 4 h in a solution of 70% water, 20% zinc acetate, and 10% acetic acid in a pressure vessel as a potential chemical recycling process. Approximately 93% yield of RO was obtained as a brown transparent viscous fluid that was found to be homogeneously miscible with the pure epoxy resin with different concentrations up to 40 wt % RO. The FTIR showed no evidence for the presence of reactive epoxy groups in the chemical structure of RO but only cured epoxy chemical groups with a high-intensity oxidation peak evaluated from the carbonyl index. The excellent miscibility of RO with epoxy resin without any chemical modification or functionalization suggested that the RO can be utilized to create thermoset materials with comparable mechanical and rheological properties to that of the pristine epoxy resin. The chemical structure of RO with no reactive groups implied that the fully cured epoxy resin/RO blends created semi-interpenetrating networks that have a thermoset epoxy resin miscible with the low molecular weight RO trapped between the network structure. It is also concluded that the RO was not copolymerized with pure epoxy resin or contributed any role in improving the cross-link structure. The η_0 for epoxy resin/RO blends was evaluated as a function of the RO content from the angular frequency dependence of η^* according to the Cross model. The η_0 showed a positive deviation from the linear mixing rule and was well described by the Lecyar model. The isothermal and nonisothermal curing kinetics for epoxy resin/RO blends of different concentrations were investigated rheologically by monitoring the change in the rheological parameters G', G'', η^*, and tan δ as a function of curing time, temperature, and angular frequency. The RO was found to have an insignificant effect on the curing kinetics, including T_{gel}, t_{gel}, and E_a. The E_a was evaluated from the temperature dependence of t_{gel} according to the Arrhenius equation and was found to be 46 ± 2 kJ/mol for all epoxy resin/RO blends, regardless of the different blend compositions. Only one tan δ peak shifted systematically to lower temperatures when increasing the content of the RO up to 40 wt % RO, indicating that the epoxy resin and the RO are miscible with a single glass-relaxation process and T_g for each blend composition. The cross-link density was determined from the plateau modulus of E' at 45 °C above the T_g according to the rubber elasticity theory and was found to decrease linearly with increasing the RO content. The RO had strongly influenced the mechanical properties of the pure epoxy resin with significant increases in the modulus by 40% and 20% for epoxy resin/RO blends with 15 and 25 wt % RO, respectively. Dramatic decreases in the elongation by −49% and −61% were also observed for 15 and 25 wt % RO, respectively. The blends with 15 and 25 wt % RO have promising mechanical behaviors that can be improved with reactive modifiers or coupling agents to be comparable to or exceed the baseline (future work).

AUTHOR INFORMATION

Corresponding Authors

Samy Madbouly − *Pacific Northwest National Laboratory, Richland, Washington 99354, United States*; orcid.org/0000-0002-4903-4362; Email: Samy.madbouly@pnnl.gov

Kevin L. Simmons − *Pacific Northwest National Laboratory, Richland, Washington 99354, United States*; Email: kl.simmons@pnnl.gov

Authors

Jose L. Ramos − *Pacific Northwest National Laboratory, Richland, Washington 99354, United States*

Wenbin Kuang − *Pacific Northwest National Laboratory, Richland, Washington 99354, United States*

Yongsoon Shin − *Pacific Northwest National Laboratory, Richland, Washington 99354, United States*

Notes

The views and opinions of the authors expressed herein do not necessarily state or reflect those of the United States Government or any agency thereof. Neither the United States Government nor any agency thereof, nor any of their employees, makes any warranty, expressed or implied, or assumes any legal

liability or responsibility for the accuracy, completeness, or usefulness of any information, apparatus, product, or process disclosed, or represents that its use would not infringe privately owned rights.

The authors declare no competing financial interest.

■ ACKNOWLEDGMENTS

This work is supported by the U.S. Department of Energy, Office of Energy Efficiency and Renewable Energy (EERE), Hydrogen and Fuel Cells Technologies Office (HFTO). Pacific Northwest National Laboratory (PNNL) is operated by Battelle Memorial Institute for the U.S. Department of Energy under Contract DE-AC06-76RLO01830. A portion of this research was performed using Environmental Molecular Science Laboratory (EMSL), a DOE Office of Science User Facility sponsored by the Office of Biological and Environmental Research. The authors would also like to thank Evonik Industries for providing materials for this project.

■ REFERENCES

(1) Verma, S., Gangil, B., Ranakoti, L.; Verma, J. Study of Physical, Thermal, and Mechanical Properties of Thermosetting Polymer Composites. In *Dynamic Mechanical and Creep-Recovery Behavior of Polymer-Based Composites*; Elsevier, 2024; pp 33−51.

(2) Gangil, B., Kumar, S., Tejyan, S., Ranakoti, L.; Verma, S. Introduction to Thermosetting Polymer Composites: Applications, Advantages, and Drawbacks. In *Dynamic Mechanical and Creep-Recovery Behavior of Polymer-Based Composites*; Elsevier, 2024; pp 11−19.

(3) Wang, T.; Xia, L.; Ni, M.; Pan, S.; Luo, C. Fundamentals of Infrared Heating and Their Application in Thermosetting Polymer Curing: A Review. *Coatings* **2024**, *14* (7), 875.

(4) Yang, J.; Bai, Y.; Sun, J.; Lv, K.; Lang, Y. Recent Advances of Thermosetting Resin and its Application Prospect in Oil and Gas Drilling and Production Engineering. *Geoenergy Science and Engineering* **2023**, *230*, No. 212222.

(5) Gül, Ç.; Kocak, E. D. Emerging Applications of Polymers for Automobile Industries. *Specialty Polymers* **2022**, 157−168.

(6) Guney Yilmaz, S.; Ferik, E.; Birak, S. B.; Ozkutlu Demirel, M.; Oz, Y.; Kaboglu, C. High-Performance Thermoplastic Nanocomposites for Aerospace Applications: A Review of Synthesis, Production, and Analysis. *Journal of Reinforced Plastics and Composites* **2024**, *22*, No. n/a.

(7) Thermoset Composites Market Demand, Scope & Challenges by 2028. *Data Bridge Market Research*, 2021. https://www.databridgemarketresearch.com/reports/global-thermoset-composites-market.

(8) Oladele, I. O.; Okoro, C. J.; Taiwo, A. S.; Onuh, L. N.; Agbeboh, N. I.; Balogun, O. P.; Olubambi, P. A.; Lephuthing, S. S. Modern Trends in Recycling Waste Thermoplastics and Their Prospective Applications: A Review. *Journal of Composites Science* **2023**, 7 (5), 198.

(9) Jung, H.; Shin, G.; Kwak, H.; Hao, L. T.; Jegal, J.; Kim, H. J.; Jeon, H.; Park, J.; Oh, D. X. Review of Polymer Technologies For Improving the Recycling and Upcycling Efficiency of Plastic Waste. *Chemosphere* **2023**, *320*, No. 138089.

(10) Wang, B.; Wang, Y.; Du, S.; Zhu, J.; Ma, S. Upcycling of Thermosetting Polymers into High-Value Materials. *Materials Horizons* **2023**, *10* (1), 41−51.

(11) Madbouly, S. A. Novel Recycling Processes for Thermoset Polyurethane Foams. *Current Opinion in Green and Sustainable Chemistry* **2023**, *42*, No. 100835.

(12) Zhang, C.; Xue, J.; Yang, X.; Ke, Y.; Ou, R.; Wang, Y.; Madbouly, S. A.; Wang, Q. From Plant Phenols to Novel Bio-Based Polymers. *Prog. Polym. Sci.* **2022**, *125*, No. 101473.

(13) Madbouly, S. A.; Lendlein, A. Degradable Polyurethane/Soy Protein Shape-Memory Polymer Blends Prepared via Environmentally-Friendly Aqueous Dispersions. *Macromol. Mater. Eng.* **2012**, *297* (12), 1213−1224.

(14) Halpern, J. M.; Urbanski, R.; Weinstock, A. K.; Iwig, D. F.; Mathers, R. T.; Von Recum, H. A. A Biodegradable Thermoset Polymer Made by Esterification of Citric Acid and Glycerol. *J. Biomed. Mater. Res., Part A* **2014**, *102* (5), 1467−1477.

(15) Cai, M.; Liu, H.; Jiang, Y.; Wang, J.; Zhang, S. A high-strength Biodegradable Thermoset Polymer for Internal Fixation Bone Screws: Preparation, in Vitro and in Vivo Evaluation. *Colloids Surf., B* **2019**, *183*, No. 110445.

(16) Jha, S.; Akula, B.; Enyioma, H.; Novak, M.; Amin, V.; Liang, H. Biodegradable Biobased Polymers: A Review of the State of the Art, Challenges, and Future Directions. *Polymers* **2024**, *16* (16), 2262.

(17) Sternberg, J.; Sequerth, O.; Pilla, S. Green Chemistry Design in Polymers Derived from Lignin: Review And Perspective. *Prog. Polym. Sci.* **2021**, *113*, No. 101344.

(18) Ochiai, B.; Yashima, M.; Soegawa, K.; Matsumura, Y. Biodegradable Epoxy Thermosetting System with High Adhesiveness Based on Glycidate-Acid Anhydride Curing. *ACS Macro Lett.* **2023**, *12* (1), 54−58.

(19) Naik, N.; Shivamurthy, B.; Thimmappa, B. H. S.; Guo, Z.; Bhat, R. Bio-Based Epoxies: Mechanical Characterization and Their Applicability in the Development of Eco-Friendly Composites. *Journal of Composites Science* **2022**, *6* (10), 294.

(20) An, W.; Liu, X.; Li, J.; Zhao, X.; Long, Y.; Xu, S.; Wang, Y. Z. Water-Solvent Regulation on Complete Hydrolysis of Thermosetting Polyester and Complete Separation of Degradation Products. *Journal of Hazardous Materials* **2023**, *453*, No. 131423.

(21) Maines, E. M.; Polley, M. A.; Haugstad, G.; Zhao, B.; Reineke, T. M.; Ellison, C. J. Mechanical Recycling of 3D-Printed Thermosets for Reuse in Vat Photopolymerization. *ACS Applied Polymer Materials* **2024**, *6* (8), 4625−4633.

(22) Liu, Y.; Yu, Z.; Wang, B.; Li, P.; Zhu, J.; Ma, S. Closed-loop Chemical Recycling of Thermosetting Polymers and Their Applications: A Review. *Green Chem.* **2022**, *24* (15), 5691−5708.

(23) Morici, E.; Dintcheva, N. T. Recycling of Thermoset Materials and Thermoset-Based Composites: Challenge and Opportunity. *Polymers* **2022**, *14* (19), 4153.

(24) Türel, T.; Dağlar, Ö.; Eisenreich, F.; Tomović, Ž. Epoxy Thermosets Designed for Chemical Recycling. *Chemistry−An Asian Journal* **2023**, *18* (15), No. e202300373.

(25) An, W.; Wang, X. L.; Liu, X.; Wu, G.; Xu, S.; Wang, Y. Z. Chemical Recovery of Thermosetting Unsaturated Polyester Resins. *Green Chem.* **2022**, *24* (2), 701−712.

(26) Zhang, Y.; Zhang, L.; Yang, G.; Yao, Y.; Wei, X.; Pan, T.; Wu, J.; Tian, M.; Yin, P. Recent advances in recyclable thermosets and thermoset composites based on covalent adaptable networks. *Journal of Materials Science & Technology* **2021**, *92*, 75−87.

(27) Krishnakumar, B.; Sanka, R. P.; Binder, W. H.; Parthasarthy, V.; Rana, S.; Karak, N. Vitrimers: Associative Dynamic Covalent Adaptive Networks in Thermoset Polymers. *Chemical Engineering Journal* **2020**, *385*, No. 123820.

(28) Podgórski, M.; Fairbanks, B. D.; Kirkpatrick, B. E.; McBride, M.; Martinez, A.; Dobson, A.; Bongiardina, N. J.; Bowman, C. N. Toward Stimuli-Responsive Dynamic Thermosets Through Continuous Development And Improvements in Covalent Adaptable Networks (CANs). *Adv. Mater.* **2020**, *32* (20), No. 1906876.

(29) Bowman, C.; Du Prez, F.; Kalow, J. Introduction to Chemistry for Covalent Adaptable Networks. *Polym. Chem.* **2020**, *11* (33), 5295−5296.

(30) Miravalle, E.; Viada, G.; Bonomo, M.; Barolo, C.; Bracco, P.; Zanetti, M. Recycling of Commercially Available Biobased Thermoset Polyurethane Using Covalent Adaptable Network Mechanisms. *Polymers* **2024**, *16* (15), 2217.

(31) Gregg, J. B.; Wilson, J. A.; Brown, S. L.; Slark, A. T. Dissociative Covalent Adaptable Networks from Unsaturated Polyesters. *Eur. Polym. J.* **2024**, *215*, No. 113195.

(32) Sahraeeazartamar, F.; Yang, Z.; Terryn, S.; Jozic, D.; Vanderborght, B.; Van Assche, G.; Brancart, J. Designing Flexible and Self-Healing Electronics Using Hybrid Carbon Black/Nanoclay

Composites Based on Diels−Alder Dynamic Covalent Networks. *Macromolecules* **2024**, *57* (2), 539−553.
(33) Vidal, J.; Hornero, C.; De la Flor, S.; Vilanova, A.; Dieste, J. A.; Castell, P. Strategies towards Fully Recyclable Commercial Epoxy Resins: Diels−Alder Structures in Sustainable Composites. *Polymers* **2024**, *16* (8), 1024.
(34) Zhao, X.; Liu, X.; Feng, K.; An, W. L.; Tian, F.; Du, R.; Xu, S.; Chen, L.; Wu, G.; Wang, Y. Z. Multicycling of Epoxy Thermoset Through a Two-Step Strategy of Alcoholysis and Hydrolysis using a Self-Separating Catalysis System. *ChemSusChem* **2022**, *15* (3), No. e202101607.
(35) Wang, B.; Wang, Y.; Du, S.; Zhu, J.; Ma, S. Upcycling of Thermosetting Polymers into High-Value Materials. *Materials Horizons* **2023**, *10* (1), 41−51.
(36) Hamel, C. M.; Kuang, X.; Qi, H. J. Modeling the Dissolution of Thermosetting Polymers and Composites Via Solvent Assisted Exchange Reactions. *Composites Part B: Engineering* **2020**, *200*, No. 108363.
(37) Manarin, E.; Boumezgane, O.; Giannino, A.; De Fabritiis, V.; Griffini, G.; Turri, S. Towards a Zero-Waste Chemcycling of Thermoset Polymer Composites: Catalyst Assisted Mild Solvolysis for Clean Carbon Fiber Liberation and Circular Coating Development. *Sustainable Materials and Technologies* **2024**, *41*, No. e01031.
(38) Vogiantzi, C.; Tserpes, K. A Preliminary Investigation on a Water-and Acetone-Based Solvolysis Recycling Process for CFRPs. *Materials* **2024**, *17* (5), 1102.
(39) Okajima, I.; Sako, T. Recycling Fiber-Reinforced Plastic Using Supercritical Acetone. *Polym. Degrad. Stab.* **2019**, *163*, 1−6.
(40) Okajima, I.; Watanabe, K.; Haramiishi, S.; Nakamura, M.; Shimamura, Y.; Sako, T. Recycling of Carbon Fiber Reinforced Plastic Containing Amine-Cured Epoxy Resin Using Supercritical and Subcritical Fluids. *Journal of Supercritical Fluids* **2017**, *119*, 44−51.
(41) DiPucchio, R. C.; Stevenson, K. R.; Lahive, C. W.; Michener, W. E.; Beckham, G. T. Base-Mediated Depolymerization of Amine-Cured Epoxy Resins. *ACS Sustainable Chem. Eng.* **2023**, *11* (48), 16946−16954.
(42) Shi, X.; He, X.; Luo, C.; Chung, C.; Ding, Y.; Yu, K. Influences of Material and Processing Conditions on the Depolymerization Speed of Anhydride-Cured Epoxy During The Solvent-Assisted Recycling. *Polymer* **2022**, *252*, No. 124964.
(43) Zhao, W.; An, L.; Wang, S. 2021. Recyclable High-Performance Epoxy-Anhydride Resins with DMP-30 as the Catalyst of Transesterification Reactions. *Polymers* **2021**, *13*, 296.
(44) Liu, T.; Zhao, B.; Zhang, J. Recent Development of Repairable, Malleable and Recyclable Thermosetting Polymers Through Dynamic Transesterification. *Polymer* **2020**, *194*, No. 122392.
(45) Shen, M.; Cao, H.; Robertson, M. L. Hydrolysis and Solvolysis as Benign Routes for the End-of-Life Management of Thermoset Polymer Waste. *Annu. Rev. Chem. Biomol. Eng.* **2020**, *11* (1), 183−201.
(46) Tortorici, D.; Clemente, R.; Laurenzi, S. Solvolysis Process for Recycling Carbon Fibers from Epoxy-Based Composites. *Macromol. Symp.* **2024**, *413*, No. 2400039.
(47) Fortunato, G.; Anghileri, L.; Griffini, G.; Turri, S. Simultaneous Recovery of Matrix and Fiber in Carbon Reinforced Composites Through a Diels−Alder Solvolysis Process. *Polymers* **2019**, *11* (6), 1007.
(48) La Rosa, A. D.; Leistad, V.; Gavric, Z. LCA of Reusing Carbon Fibers Recycled Through Solvolysis Process of Thermoset Composites. *Role of Circular Economy in Resource Sustainability* **2022**, 143−153.
(49) DiPucchio, R. C.; Stevenson, K. R.; Lahive, C. W.; Michener, W. E.; Beckham, G. T. Base-Mediated Depolymerization of Amine-Cured Epoxy Resins. *ACS Sustainable Chem. Eng.* **2023**, *11* (48), 16946−16954.
(50) Barcenas, L.; Narayana, S. S.; Khoun, L.; Trudeau, P.; Hubert, P. Thermochemical and Rheological Characterization of Highly Reactive Thermoset Resins for Liquid Molding. *Journal of Composite Materials* **2023**, *57* (19), 3013−3024.
(51) Madbouly, S. A.; Otaigbe, J. U. Rheokinetics of Thermal-Induced Gelation of Waterborne Polyurethane Dispersions. *Macromolecules* **2005**, *38* (24), 10178−10184.
(52) Madbouly, S. A.; Ougizawa, T. Rheological Investigation of Shear Induced-Mixing and Shear Induced-Demixing for Polystyrene/Poly (Vinyl Methyl Ether) Blend. *Macromol. Chem. Phys.* **2004**, *205* (9), 1222−1230.
(53) Wang, T.; Xia, L.; Ni, M.; Pan, S.; Luo, C. Fundamentals of Infrared Heating and Their Application in Thermosetting Polymer Curing: A Review. *Coatings* **2024**, *14* (7), 875.
(54) Alam, T. M.; Jones, B. H. Investigating Chain Dynamics in Highly Crosslinked Polymers using Solid-State 1H NMR Spectroscopy. *J. Polym. Sci., Part B: Polym. Phys.* **2019**, *57* (17), 1143−1156.
(55) Madbouly, S. A.; Ougizawa, T. Binary Miscible Blends of Poly(Methyl Methacrylate)/Poly (A-Methyl Styrene-Co-Acrylonitrile): I. Rheological Behavior. *Journal of Macromolecular Science, Part B* **2002**, *41* (2), 255−269.
(56) Abali, B. E.; Yardımcı, M. Y.; Zecchini, M.; Daissè, G.; Marchesini, F. H.; De Schutter, G.; Wan-Wendner, R. Experimental Investigation for Modeling the Hardening of Thermosetting Polymers During Curing. *Polym. Test.* **2021**, *102*, No. 107310.
(57) Fisher, A.; Radhakrishnan, A.; Levy, A.; Teuwen, J.; Kratz, J. Effect of Pre-Curing on Thermoplastic-Thermoset Interphases. *Journal of Composite Materials* **2024**, *58*, No. 2713.
(58) Chen, C.; Poursartip, A.; Fernlund, G. Cure-Dependent Microstructures and Their Effect on Elastic Properties of Interlayer Toughened Thermoset Composites. *Composites science and technology* **2020**, *197*, No. 108241.
(59) Liu, T.; Zhao, B.; Zhang, J. Recent Development of Repairable, Malleable and Recyclable Thermosetting Polymers Through Dynamic Transesterification. *Polymer* **2020**, *194*, No. 122392.
(60) Haring, A. P.; Singh, M.; Koh, M.; Cesewski, E.; Dillard, D. A.; Kong, Z.; Johnson, B. N. Real-Time Characterization of Hydrogel Viscoelastic Properties and Sol-Gel Phase Transitions Using Cantilever Sensors. *J. Rheol.* **2020**, *64* (4), 837−850.
(61) Suman, K.; Shanbhag, S.; Joshi, Y. M. Phenomenological Model of Viscoelasticity for Systems Undergoing Sol−Gel Transition. *Phys. Fluids* **2021**, *33* (3), No. 033103.
(62) Hao, C.; Zhao, B.; Shao, L.; Cao, Y.; Fei, M.; Liu, W.; Liu, T.; Chang, Y. C.; Simmons, K. L.; Zhang, J. Mild Chemical Recycling of Carbon Fiber-Reinforced Epoxy Composites in Aqueous Buffers and Development of Hydrothermally Recyclable Vitrimer Composites From Recyclates. *Resources, Conservation and Recycling* **2024**, *207*, No. 107668.
(63) Gonzalez-Garzon, M.; Shahbikian, S.; Huneault, M. A. Properties and Phase Structure of Melt-Processed PLA/PMMA Blends. *Journal of Polymer Research* **2018**, *25*, 1−13.
(64) Kalogeras, I. M.; Brostow, W. Glass Transition Temperatures in Binary Polymer Blends. *J. Polym. Sci., Part B: Polym. Phys.* **2009**, *47* (1), 80−95.
(65) Zhang, X.; Zhao, Y.; Xia, H.; Ao, X.; Liu, J.; Zhou, J.; Wang, Y. Modeling of Curing and Post-Curing Kinetics For a Thermoset Adhesive. *Thermochim. Acta* **2024**, *736*, No. 179745.
(66) Loban, O. I.; Olikhova, Y. V.; Gorbunova, I. Y.; Kostromina, N. V. Curing Rheokinetics of Epoxy-Amine Composition. *Thermochim. Acta* **2024**, *740*, No. 179825.
(67) Bashir, M. A. Cure Kinetics of Commercial Epoxy-Amine Products with ISO-Conversional Methods. *Coatings* **2023**, *13* (3), 592.
(68) Madbouly, S. A.; Otaigbe, J. U.; Nanda, A. K.; Wicks, D. A. Rheological Behavior of Aqueous Polyurethane Dispersions: Effects of Solid Content, Degree of Neutralization, Chain Extension, and Temperature. *Macromolecules* **2005**, *38* (9), 4014−4023.
(69) Madbouly, S. A. Binary Miscible Blends of Poly(Methyl Methacrylate)/Poly(α−Methyl Styrene-Co-Acrylonitrile). IV. Relationship Between Shear Flow and Viscoelastic Properties. *Journal of Macromolecular Science, Part B* **2003**, *42* (6), 1209−1223.
(70) Madbouly, S. A.; Xia, Y.; Kessler, M. R. Sustainable Polyurethane−Lignin Aqueous Dispersions and Thin Films: Rheological

Behavior and Thermomechanical Properties. *ACS Applied Polymer Materials* **2020**, *2* (11), 5198−5207.